Excited-level lifetimes and hyperfine-structure measurements on ions using collinear laser–ion-beam spectroscopy

Jian Jin* and D. A. Church
Physics Department, Texas A&M University, College Station, Texas 77843
(Received 19 August 1993)

The mean lifetimes τ of the Ca II $4p\,^2P_{1/2}$ and $4p\,^2P_{3/2}$ levels, and the ^{35}Cl II $4p'\,^1F_3$ level, have been measured by a variant of the collinear laser–ion-beam lifetime technique applied previously to the Ar II $4p'\,^2F^o_{7/2}$ level [Jian Jin and D. A. Church, Phys. Rev. A **47**, 132 (1993)]. The present results are τ(Ca II, $4p\,^2P_{1/2}$)=7.098(0.020) ns, τ(Ca II, $4p\,^2P_{3/2}$)=6.924(0.019) ns, and τ(Cl II, $4p'\,^1F_3$) =11.17(0.06) ns. The experimental lifetimes of these, plus the Ar II $4p'\,^2F_{7/2}$ level, are compared with available recent many-electron calculations. Typically 1%–3% differences between measurement and *ab initio* theory are found, while certain semiempirical calculations are in better agreement with experiment. Data for other precise lifetime measurements on alkali-metal systems are compared with recent *ab initio* and semiempirical calculations to provide perspective on the Ca II results. The hyperfine structure of the ^{35}Cl II $3d'\,^1G_4$–$4p'\,^1F_3$ transition was also measured and analyzed in the course of the measurements, with the resulting hyperfine-structure constants: $A(^1F_3)$=301.9(0.5) MHz, $B(^1F_3)$=−6.7(0.8) MHz, $A(^1G_4)$=205.1(0.5) MHz, and $B(^1G_4)$=−3.9(2.4) MHz.

PACS number(s): 32.70.Fw, 31.30.Gs, 31.20.Di, 31.20.Gm

I. INTRODUCTION

Careful laser-ion excitation measurements of selected atomic levels can provide mean lifetime data with accuracies and precisions exceeding 0.5% [1–5]. The use of a laser beam for excitation guarantees the absence of optical cascades into the level of interest, a primary error source in less selective techniques [6], while the employment of ions in a fast beam accurately defines a time scale in the nanosecond range. A major motivation for such precise measurements is the continued improvement in accuracy of many-electron theoretical calculations. Many level lifetimes have been calculated using improved techniques [7–9] but accuracies are often difficult to estimate when comparisons with precise and accurate experimental results are not feasible. Since lifetime information is important in the analysis of processes in astrophysical and fusion plasmas [10], an assessment of the expected accuracy of the available theory is desirable. For the case of a single electron outside closed shells in a heavy, many-electron atom such as Cs, a combination of accurate theory [11] and experiment [12] could result in the determination of the coupling constants of the electroweak interaction.

For the light alkali-metal atoms Li and Na, with a single electron outside closed shells, the most precise experimental results for the P-state lifetimes[1] lie about six standard deviations of the experimental error above the most recent theoretical calculations [13]. A comparison of various calculations by different groups reveals better internal agreement between different theoretical approaches than between experiment and theory [14]. This is particularly disturbing for the relatively simple (for theory) case of the Li $2p\,^2P_{1/2}$. Oscillator strengths, obtained by several different calculation methods [15] which account for core polarization and intershell correlation, agree within about 0.1% [16]. The significant disagreement with experiment may be an indication of systematic problems either with the theory or with experimental techniques. In general, the theory tends to predict faster decays than are observed, for the few transitions of light atoms in which comparison is possible, but better agreement between experiment and theory occurs for the Cs $^2P_{1/2}$ level [17] and the theoretical lifetime lies above the experimental values for the $6p\,^2P_{1/2}$ level [13] of Ba^+. To provide supporting information for further precise comparisons between experiment and theory, we have measured the lifetimes of both $4p\,^2P$ levels of the intermediate-Z ion Ca II, which has a single electron outside closed shells. A level of Cl II, which has two holes in a closed shell, was also studied to determine the effectiveness of the experimental method on a system with hyperfine structure. Results of our earlier measurement on Ar II, which has a single hole in a closed shell, are also discussed in the context of comparisons of recent theory with experiment for intermediate-Z ions, when the experimental results are supported by at least two different measurements which agree. Both the Ar II and Cl II states also have core excitation. Isotopes without nuclear spin were used in the measurements on Ca II and Ar II, to avoid the complications introduced by hyperfine structure. Both common isotopes of Cl II have nuclear spin, however, so the hyperfine spectrum of the $3d'\,^1G_4$–$4p'\,^1F_3$ transition was also studied. The grouping of the hyperfine transitions permitted excitation for the lifetime measurement, but with lower precision compared to the other ion data. The hyperfine structure has

*Present address: Lawrence Berkeley Laboratory, Berkeley, CA 94720.

been analyzed to obtain the A and B hyperfine constants for the upper and lower levels. The data are compared with similar results for the Cl II $3d'\,^3G_5-4p'\,^3F_4$ transition [18,19].

II. EXPERIMENTAL OVERVIEW

The experimental method has been discussed in some detail in earlier publications [2,5,20], but a brief synopsis of the general technique in this section, and a discussion in Sec. III of differences with our earlier measurement [5] and further improvements in technique, are appropriate.

A beam of ions from an electrostatic accelerator, with selected momentum-to-charge ratio, was carefully collimated and superimposed on the path of a counterpropagating fixed-frequency laser beam. The cw laser beam was produced by a passively stabilized single-mode ring dye laser pumped by an argon-ion laser. The mode structure of the laser beam, and its wavelength, were continuously monitored. The laser was initially tuned to a fixed wavelength, which could be further tuned using the Doppler effect of the moving ions, to excite a transition originating from a metastable level of the ion. This level was populated at a few tenths of a percent in the ion source.

A weak uniform electric field E parallel to the beams was produced in a limited spatial region by a fixed potential difference across any array of plates, called a Doppler scanning system (DSS). The potential of the DSS as a whole could be adjusted relative to grounded reference planes. The changing Doppler shift of the ions in the constant electric field limited the resonant excitation of the metastable ions to a small spatial region, which could be scanned along the beam by ramping the DSS potential. A fixed optical detection system accepted time-delayed photons from ions excited upbeam. A time scale of nanoseconds was determined by the ion velocity, which in turn was controlled by the applied potentials according to $\Delta t=(2m/q)^{1/2}E^{-1}(U_A^{1/2}-U_B^{1/2})$ where U_A and U_B are two potentials applied to the DSS. By this means, photons from an exponential decay of the excited level were observed vs potential U, which was accurately converted to a time difference. Examples of the resulting optical decay signals from the $4p'\,^1F_3$ level of Cl II and the $4p\,^2P_{1/2}$ level of Ca II appear in Fig. 1. The energy-level diagrams in Fig. 2 illustrate the excitation schemes used to produce these signals. In all cases, the monitored decays occurred at wavelengths well separated from the excitation wavelength, minimizing problems with scattered light.

To scan a spectrum, the electric field was reduced to zero during the voltage ramp of the DSS, resulting in uniform excitation of the metastable ions within the plates.

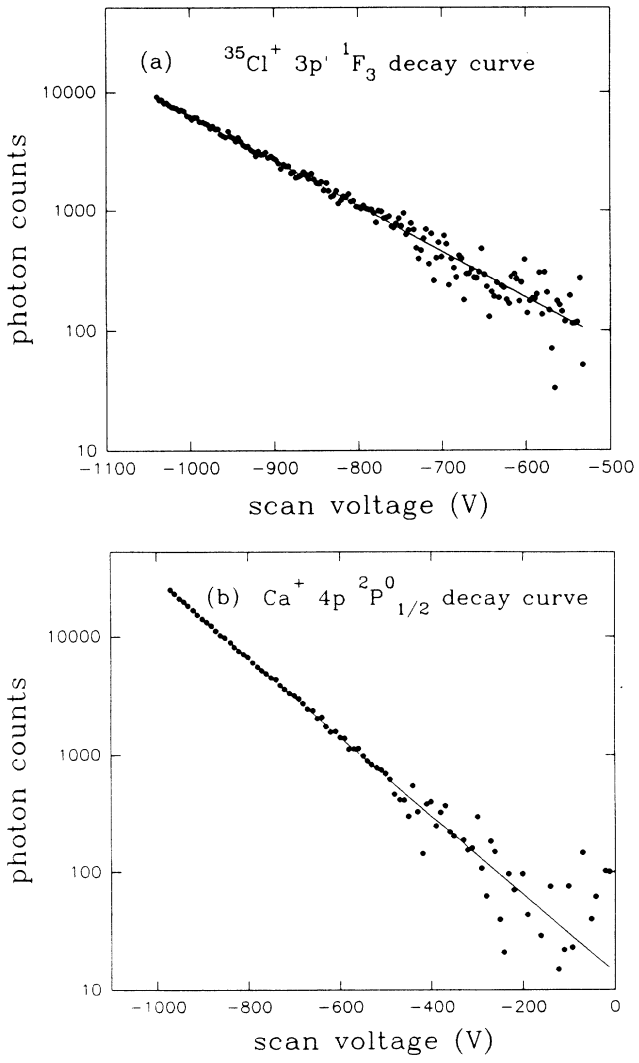

FIG. 1. (a) Logarithm of the intensity of the optical decay of the $4p'\,^1F_3$ level of Cl II vs voltage applied to the Doppler scanning system. (b) A similar plot for the $4p\,^2P_{1/2}$ level of Ca II.

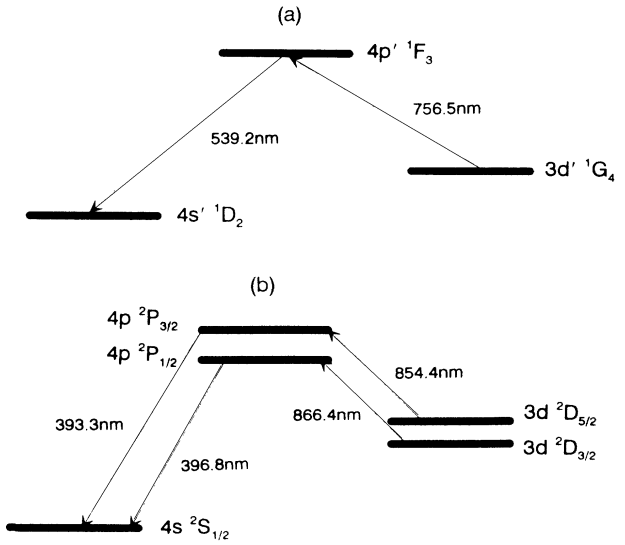

FIG. 2. (a) Partial energy-level diagram of Cl II, showing the exciting transition from the $^1G_4$ metastable level and the optical decay that was monitored. (b) A similar diagram for Ca II. The $^2P_{1/2}$ and $^2P_{3/2}$ levels were studied.

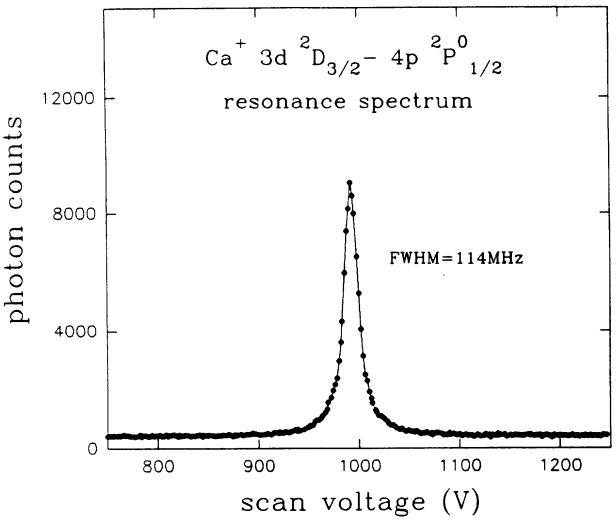

FIG. 3. Scan of the spectrum of the Ca II $3d\,^2D_{3/2}-4p\,^2P_{1/2}$ transition.

The observed intensity variations now appear as a function of Doppler-tuned wavelength or frequency. The resulting spectrum was slightly asymmetric, since ions excited upbeam could still decay with a time delay into the acceptance solid angle of the optical detection system. A spectral scan showing the Ca II $^2P_{1/2}$ line appears in Fig. 3. The resolution is limited to about 120 MHz by the distribution of ion velocities in the source, the natural width of the transition, and by the 30-MHz laser linewidth.

The collinear beam arrangement, and Doppler tuning of the local ion velocity by potential changes, constitute the primary advantages of this technique, since neither changes in ion source or beam transport operating conditions, nor frequency or spatial scanning of the dye laser, are required for lifetime or spectral measurements. The inherent stability of the measurement system favors signal averaging.

III. APPARATUS AND TECHNIQUE

Many details of the apparatus, including the accelerator and laser systems, and the design and test of the electric-field plates, have been discussed in Ref. [5], and need not be repeated here. Instead, changes in operating conditions pertinent to these measurements are described, including recent improvements in the apparatus.

The Cl^+ beam was developed by discharging CCl_4 vapor in the source. The vapor above liquid CCl_4 was admitted through a needle valve. Deposits on the anode and filament were observed to accumulate, gradually reducing electron emission, and reducing beam current. Filament replacement after 3–4 h of operating time increased the statistical uncertainty of the Cl^+ measurements relative to measurements with other ions.

To obtain the Ca^+ beam, a constant flow of neon gas was maintained to stabilize the discharge plasma. Ca metal was sputtered by the neon ions, with a rate which was controlled by adjusting the discharge current. A stable Ca^+ beam lasting more than 20 h resulted. The extraction potential was increased from 30 to 50 kV for the Ca^+ measurements, to extend the spatial decay lengths of the Ca II levels, which have slightly shorter lifetimes.

The finite mass resolution of the bending magnet of our accelerator system was insufficient to completely resolve isotopic beams of Ca^+ or Cl^+. However, each isotopic mass had a different velocity, and hence Doppler shift, following subsequent acceleration to and within the DSS. Consequently ion isotopes other than the dominant isotope had significantly different Doppler tunings, as well as different spectra due to the isotope effect, and could not be excited even if inadvertently in the beam.

A PY-2 dye was used to excite the near-infrared transition of Cl II. The laser optics were changed when using the infrared Styryl 9M dye required for the Ca II transitions. Temperature control of this dye limited laser focus changes, and the dye circulator was not deactivated during the whole sequence of measurements, to inhibit problems like dye splashing and mode hops due to dye crystallization. A He-Ne laser beam was used to aid in the alignment of the infrared laser beam through the collimating apertures.

The measured optical decay signal was also normalized to the ion-beam current and laser power. A separate photomultiplier tube monitored the nonresonant background of scattered light due to ion-residual gas collisions, about 40 counts/s μA of beam current at a typical residual pressure. Laser power fluctuations were monitored with a laser power meter. Since both ion beam and laser were operated with constant parameters, few fluctuations larger than about 2% were observed. No significant differences in the mean lifetimes determined with or without normalization were found.

Due to the hyperfine interaction, the spectrum of the Cl II $3d'\,^1G_4-4p'\,^1F_3$ transition was relatively complex

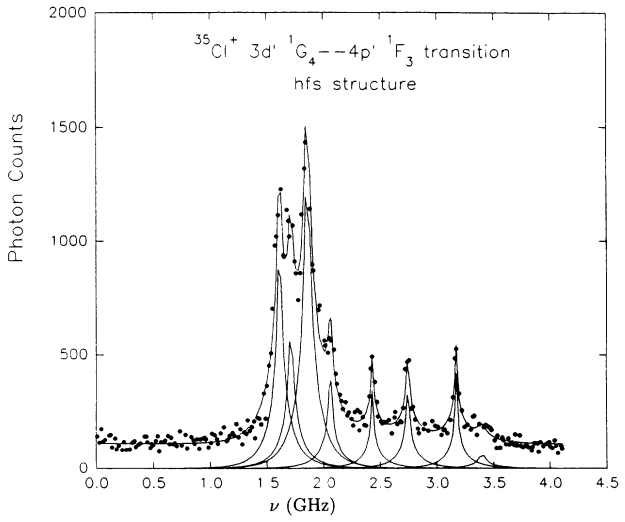

FIG. 4. Scan of the spectrum of the $3d'\,^1G_4-4p'\,^1F_3$ transition of ^{35}Cl II. The multiple lines due to the hyperfine structure have been fitted by Voigt functions. The "flag" of $\Delta F=-1$ transitions are bunched at the lower frequencies, with intensities departing from the statistical weights.

TABLE I. The systematic corrections and random errors associated with the Ca II and Cl II lifetime measurements.

Source	Correction (units of 10^{-3})	Error (units of 10^{-3})
Residual gas collisions	+0.33 (Cl II)	±0.33 (Cl II)
	+0.11 (Ca II)	±0.11 (Ca II)
Electric field E		±2.0
Alignment of ion beam and E field	+0.44	±0.44
Determination of resonance potential U		±0.86
Stark effect		negligible
Quantum beats		±2 (Cl II)
		negligible (Ca II)
Statistics		±4 (Cl II)
		±1.6 (Ca II)
Total	+0.77 (Cl II)	±5 (Cl II)
	+0.55 (Ca II)	±2.7 (Ca II)
	(in sum)	(in quadrature)

(see Fig. 4 in Sec. III). Within the available resolution, several of the relatively strong $\Delta F=-1$ transitions partially overlapped, permitting excitation of several transitions of the group at the wavelength of the peak of the most intense transition, during the lifetime measurements. Coupling to other ion levels can affect the lifetime of individual hyperfine transition components, so the lifetime result reported here for the Cl II $^1F_3$ level should be interpreted as a representative value nominally associated with the $F=\frac{9}{2}\rightarrow F=\frac{7}{2}$ hyperfine component, which was observed to be the most intense.

Table I lists the systematic corrections and random errors associated with the Ca II and Cl II lifetime measurements. A general discussion of errors appears in Ref. [5]. Rates of quenching collisions with residual gas depend on the background pressure ($<10^{-6}$ Torr) and on the collision cross sections. The mean quenching cross section determined experimentally [21] for Ar II states, $\bar{\sigma}=2\times10^{-14}$ cm^2, has been applied to the Cl II and Ca II measurements as well, with the assumption that the actual cross sections will not differ significantly from these values at the velocities employed. A systematic correction to each lifetime was included in the final result, with an equal magnitude of random error due to the approximate nature of the corrections.

When the excited level is oriented or aligned, quantum beats in the detected intensity of the fluorescence can lead to errors in the lifetime determination, if not included in the fitting procedure. Since the laser light was elliptically polarized, alignment or orientation could potentially occur. These moments could precess in the ambient magnetic field of the laboratory, causing quantum beats. Possible quantum beat effects at the 0.2% level were noted in the Ar II measurements. For the Ca II measurements, the chamber enclosing the DSS was wrapped in μ metal, resulting in a reduction of the ambient magnetic field by a factor near 100, to $\approx5\times10^{-3}$ g, making potential quantum beat effects on the lifetimes negligible.

IV. HYPERFINE-STRUCTURE MEASUREMENT

The ^{35}Cl II spectrum was scanned by sweeping the potential U, with the electric field set to zero. The laser beam was relatively intense, in order to observe the weaker transitions. ^{35}Cl II has a nuclear spin $I=\frac{3}{2}$, which couples to the orbital angular momentum of each excited singlet state. It is known from measurements on neighboring triplet states that the hyperfine coupling coefficient A associated with the nuclear magnetic dipole moment is much larger than the coefficient B associated with the nuclear electric quadrupole moment. Consequently, the four relatively intense $\Delta F=-1$ transitions appear as a group at the lower frequencies of the fitted spectrum (Fig. 4). The relative intensities of these transitions did not occur in the expected ratios of the statistical weights, if the $|A|\gg|B|$ condition was used to identify the transitions. However, consistent values for A and B were obtained using this condition when spectral line positions were fitted. The variation from the statistical ratios of the relative transition intensities for the strongest transitions is thought to be associated with optical pumping of the hyperfine levels during the spectral scan.

Three $\Delta F=0$ transitions appear in the midfrequency range of Fig. 4. At the higher frequencies, only the $F=\frac{5}{2}\rightarrow F=\frac{7}{2}$ transition of the two weak $\Delta F=+1$ transitions was observed, due to a premature termination of the scan. The spectrum was fitted using Voigt functions. The linewidth was held fixed for all transitions. After the spectrum was fitted, and the centroids of the peaks determined, the A and B coefficients were calculated from the measured relative frequencies using the standard hyperfine-structure equations. The results are $A(^1F_3)=301.9(0.5)$ MHz, $B(^1F_3)=-6.67(0.8)$ MHz, $A(^1G_4)=205.1(0.5)$ MHz, and $B(^1G_4)=-3.9(2.4)$ MHz. The relationships of the measured A and B coefficients to the nuclear moments are beyond the scope of this work, but have been analyzed [18,19] for the related triplet levels $3p^3(^2D)\,4p\,^3F_4$ and $3p^3(^2D)\,3d\,^3G_5$. The A and B coefficients for these levels had magnitudes comparable to our data for the singlet levels.

V. DISCUSSION

Lifetime measurements in Ar II have importance because of the extensive employment of this ion in lasers. The mean of length and velocity forms of recent

configuration interaction calculations [22] of certain Ar II $3p^4 4p$ quartet level lifetimes were within 2% of the highest precision lifetime measurement [23]. Further measurements on the Ar II $4p$ doublet levels [24] were previously compared with earlier (pre-1980) calculations. Closest agreements were found with calculations in which configuration interaction was taken into account by introducing effective operators [25]. The radial part of the line strength was obtained using the parametrized central field method. The dipole length and velocity forms of the calculations differed by about 9% for the $4p'\,^2F_{7/2}$ level, with the dipole velocity form about 3% lower than the experimental lifetime. In more recent unpublished configuration-interaction calculations, the lifetime results for this level were 8.66 (velocity) and 8.48 ns (length) [26]. The mean lies about 2% above the two experimental lifetimes. If a measure of the uncertainty in the calculations is taken as one-half the difference of the length and velocity results, than the length form of the calculation is within one standard deviation of the experimental data.

The $4p$ state lifetimes of Ca II have astrophysical importance, and are the subject of many recent calculations. *Ab initio* multiconfiguration Hartree-Fock (MCHF) and *ab initio* and semiempirical Hartree-Fock core-polarization model-potential calculations for these lifetimes have just been published by Vaeck, Godefroid, and Froese Fischer [27]. A relativistic many-body perturbation theory (MBPT) calculation, with a semiempirical correction, has been completed by Guet and Johnson [13]. A semiempirical calculation based on nonrelativistic Hartree-Fock-Slater wave functions was completed by Theodosiou [28], and the Coulomb approximation method and a model-potential method were compared for several systems, including Ca II, by Laughlin [29], within the last two years. This high level of theoretical interest indicates the importance attached to Ca II as a testing ground for advanced theoretical methods. Core-valence correlation is large in Ca II, which has a single electron outside closed shells.

In the MCHF method [27], an "all-electron" approach treated this core-valence interaction by explicit configuration interaction. Only correlation with the (outer) $3p^6$ core was included, based on earlier experience with potassium. Each pair formed by coupling one $3p$ core electron to the valence electron was treated separately. The core orbitals were obtained in two different ways, labelled MCHF-CV_1 for a HF calculation, including the core-valence correlation, for the $3p^6\,^1S$ Ca^{2+} ion core, and MCHF-CV_2 for a MCHF calculation for the ion which included the dominant radial correlation effects $3p^6 + 3p^5 4p\,^1S$. In both types of calculation, all the orbitals outside the core were varied. In a third approach, called MCHF-CV_3, first-order contributions to the transition-matrix elements from the $1s^2 2s^2 2p^6 3s^2$ core were separately determined for the $3s$ and $2p$ shells, using the MCHF-CV_2 variational wave function, and included in the final gf calculations. Lifetimes were obtained by the latter method using length and velocity forms of the matrix elements.

The core-valence correlation was also treated by incorporating the corrections to the HF theory in terms of an effective core-polarization potential with a cutoff radius r_c. This correction affects both the energy and the radial distribution of the valence electron. In the valence-core polarization (VCP) method, the core polarization was included variationally with an *ab initio* value of the cutoff radius. In the semiempirical core-polarization (SECP) approximation, core polarization was included variationally, but values of r_c were determined semiempirically. These values all resulted in a larger SECP core-polarization correction compared to the *ab initio* approach. Lifetimes of the Ca II $4p\,^2P$ levels obtained by Vaeck, Godefroid, and Frose Fischer [27] using these calculational methods appear in Table II.

Guet and Johnson [13] evaluated transition amplitudes through third order in perturbation theory. Dirac-Hartree-Fock equations were solved for the valence orbitals and eigenvalues. First-order transition amplitudes were found by evaluating reduced matrix elements of the dipole operator. Second-order calculations gave core-polarization corrections to the first-order amplitudes. The second-order transition amplitude was determined with a sum over all occupied core states and positive-energy excited states, and included higher-order (random-phase approximation) core-polarization corrections. The third-order correction included only the dominant Brueckner orbital terms. The theoretical transition amplitude was the sum of the three orders. In a semiempirical correction, the valence-electron self-energy operator was scaled to give the experimental correlation energy. It has been noted that for Ca^+, agreement of the

TABLE II. A comparison of experimental and *ab initio* theoretical lifetimes. (L) and (V) denote length and velocity forms of the matrix elements.

Level	Lifetime (ns) Experiment	Theory
Ar II $4p'\,^2F^o_{7/2}$	8.410 (0.03)[a]	8.15 (V)[b]
	8.414 (0.025)[c]	8.48 (L)[d]
		8.66 (V)[d]
Ca II $4p\,^2P_{1/2}$	7.07 (0.07)[e]	6.94[f]
	7.098 (0.020)[g]	6.83 (L)[h]
		6.78 (V)[h]
		7.045[i]
Ca II $4p\,^2P_{3/2}$	6.87 (0.06)[e]	6.75[f]
	6.924 (0.019)[g]	6.64 (L)[h]
		6.72 (V)[h]
		6.852[i]
		6.81[j]
		6.67[j]

[a]Reference [4].
[b]Reference [25].
[c]Reference [5].
[d]Reference [26].
[e]Reference [30].
[f]Reference [13], including semiempirical correction.
[g]This work.
[h]Reference [27].
[i]Reference [28].
[j]Reference [29], Coulomb approximation and model potential results.

calculation with experiment is actually improved if this correction is omitted [27]. The semiempirical correction increases the dipole transition amplitude and lowers the calculated lifetime, which improved the agreement with the experimental p-state lifetimes of Sr^+ and Ba^+.

Theodosiou [28] used a different model potential for the Ca^+ core, with a cutoff radius equal to the calculated Hartree-Slater Ca^+ core radius. This value is about twice that of the VCP approximation mentioned above. Experimental energy levels, and a theoretical static core polarizability obtained using the relativistic random-phase approximation, were employed. The lifetimes (Table II) are very close to the experimental values.

Laughlin [29] solved the Coulomb approximation equations numerically, and used a modified form of the dipole operator which emphasized large distances. He also used a model-potential approach with a dipole operator which included core-polarization effects. His calculations applied to Na, K, and Mg^+, as well as to Ca^+.

It is also useful to discuss briefly the measurement technique used in the other precise Ca II lifetime measurements, by Gosselin, Pinnington, and Ansbacher [30]. They excited the $4s$-$4p$ resonance lines using a pulsed, excimer-pumped dye laser beam, with an intensity of 200 kW cm^{-2}. The fluorescence near 850 nm to the $3d\ ^2D$ states was observed to reduce background. A crossed laser-ion-beam geometry was employed with a movable detection system carriage. Stray magnetic fields were partially compensated for by using helmholtz coils. Thus, despite the basic similarities associated with use of ion and laser beams, the earlier measurements differed in many important experimental details from the technique reported here. The agreement between the different techniques, within a single standard deviation of the least precise measurement, for each level lends some additional confidence in the experimental procedures.

In Table II one sees that the *ab initio* MCHF and MBPT theoretical lifetimes for the Ca II $^2P_{3/2}$ level lie 2–3 % below the measurements, but agree with each other to within $\pm 0.5\%$, when the least accurate of the length or velocity forms of the MCHF calculation [27] are disregarded. For the Ca II $^2P_{1/2}$ level, the calculations lie 1.7–3.7 % below the data, but agree with each other to within $\pm 1\%$. Thus agreement between different types of *ab initio* calculations is superior to agreement with experiment. Since there are no simple or straightforward ways of evaluating the accuracy of multiconfiguration calculations, intercomparisons with other theoretical calculations are often used in the absence of experiment to establish accuracy. The MBPT lifetimes in Table II include the semiempirical correction which improved agreement with 1% measurements on Sr^+, Cs, and Ba^+. However, the lifetimes without these correction are 6.98 and 6.79 ns for the Ca II $^2P_{1/2}$ and $^2P_{3/2}$ levels, respectively, in better agreement with experiment for this ion [27]. The semiempirical lifetimes obtained by Theodosiou [28] are in best agreement with the measurements, significantly better than either Laughlin's approximations [29] or the *ab initio* calculations. It is noteworthy that all theoretical calculations predict faster decays than are observed for Ca^+.

To examine the question whether these relations between experiment and theory are isolated occurrences, or part of a trend for related systems, the most precise ($\lesssim 1\%$) lifetime measurements for systems with a single electron outside a closed shell are compared with recent *ab initio* and semiempirical calculations for these systems, where high accuracy has been a goal. These are presented in Table III. In several cases, there are only single measurements at the 1% level, but in most cases the measurements are supported by further results with comparable precision. In general, less recent calculations have lower accuracy (see the references to the recent theoretical papers). An abbreviated version of Table III has been previously published [31], which listed only the highest precision measurements ($\lesssim 0.3\%$), and consequently excluded several transitions. For the heavier systems, the most precise lifetime measurements are typically at the 1% level, with the exception of the Ba II $6p\ ^2P_{3/2}$ level, and have often not yet been confirmed by measurements of comparable precision. Figure 5 shows graphically the relationship of the most precise measurements to recent theory.

The agreement of *ab initio* theory with experiment is in most cases adequate at the 1% level, but deviations of 2–3 % occur for the $4p$ levels of both Ca II and Cu I.

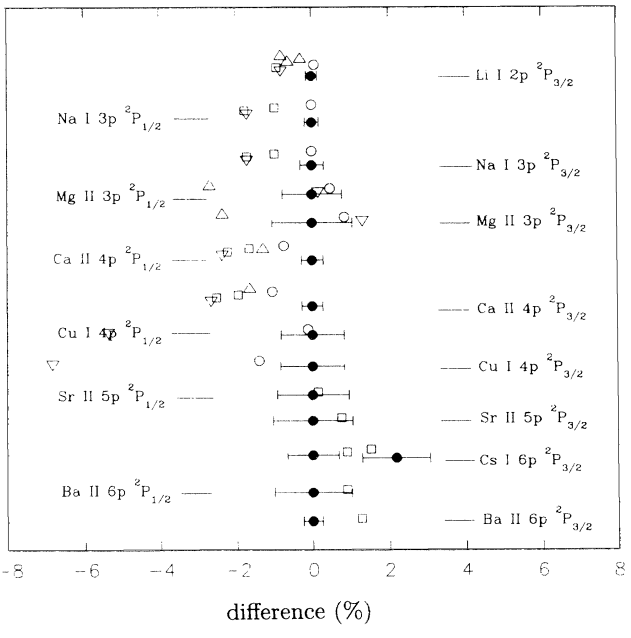

FIG. 5. A graphical presentation of the relationship of the most precise lifetime measurements from Table III, with experimental error estimates, and the results of theoretical calculations, plotted as a percent difference from experiment. The semiempirical CAHS calculations typically are in best agreement with the lifetime data. The *ab initio* theories tend to fall below experiment for the fewer-electron systems.

When the measurements are more precise, significant deviations between theory and experiment begin to appear for Li I, Na I, and Ba II as well. For the fewer-electron systems, *ab initio* theory falls below the measurements in all cases, but for Sr II, Cs I, and Ba II the measured lifetimes either agree with theory at the 1% level, or lie below theory.

The many *ab initio* calculations of the Li I $2p\ ^2P_{1/2}$ oscillator strength [8,15,16,32–36] are within a standard deviation of the 0.7% measurement of Carlsson and Sturesson [36], but disagree by several standard deviations with the five-times more precise measurement of Gaupp, Kuske, and Andrä [1]. This disagreement is the most difficult to understand from the theoretical viewpoint. For the case of Na I $3p\ ^2P_{1/2}$, the precise measurement by Gaupp, Kuske, and Andrä [1], using the same technique, has been confirmed by two independent measurements [37,38]. The least precise of these confirming measurements still lies about two standard deviations above the longest *ab initio* lifetime calculation.

The satisfactory agreement of two different MBPT calculations [11,39] with the recent measurement of the Cs I $6p\ ^2P_{1/2}$ lifetime [17] is decreased if the semiempirical correction, called into question by our Ca^+ measurements, is not used.

In contrast to the *ab initio* theoretical results, the semiempirical calculations of Theodosiou and co-workers [9,28,40] (listed under CAHS in Table III and Fig. 5) are in excellent agreement with even the most precise measurements for few-electron systems, with the largest devi-

TABLE III. A comparison of the most precise ($\leq 1\%$) lifetimes (in ns) for systems with a single electron outside of a closed shell with recent *ab initio* and semiempirical calculations.

		Theory			
Level	Experiment	MCHF	MBPT	CAHS	Other
Li I $2p\ ^2P_{1/2}$	27.29 (0.04)[a]	27.07[b]	27.04[c]	27.31[d]	27.12[e]
	27.20 (0.20)[f]				27.21[g]
					27.07[h]
Na I $3p\ ^2P_{1/2}$	16.40 (0.03)[a]	16.12[b]	16.11[c]	16.40[i]	
	16.40 (0.05)[j]		16.24[k]		
	16.38 (0.08)[l]				
Na I $3p\ ^2P_{3/2}$	16.35 (0.05)[j]	16.07[b]	16.07[c]	16.35[i]	
	16.36 (0.20)[l]		16.19[k]		
Mg II $3p\ ^2P_{1/2}$	3.854 (0.03)[m]	3.86[n,o]		3.872[i]	3.75[p]
Mg II $3p\ ^2P_{3/2}$	3.810 (0.04)[m]	3.86[n,o]		3.842[i]	3.72[p]
Ca II $4p\ ^2P_{1/2}$	7.098 (0.020)[q]	6.93[r]	6.94[s]	7.045[t]	
	7.07 (0.07)[u]		6.98[v]		
Ca II $4p\ ^2P_{3/2}$	6.924 (0.019)[q]	6.74[r]	6.75[s]	6.852[t]	6.81[w]
	6.87 (0.06)[u]		6.79[u]		
Cu I $4p\ ^2P_{1/2}$	7.26 (0.06)[x]	6.87[y]		7.251[i]	
Cu I $4p\ ^2P_{3/2}$	7.17 (0.06)[x]	6.68[y]		7.069[i]	
Sr II $5p\ ^2P_{1/2}$	7.47 (0.07)[z]		7.48[s]		
Sr II $5p\ ^2P_{3/2}$	6.69 (0.07)[z]		6.74[s]		
Cs I $6p\ ^2P_{3/2}$	30.55 (0.27)[aa]		30.82[bb]		
	29.9 (0.2)[cc]		31.01[dd]		
Ba II $6p\ ^2P_{1/2}$	7.92 (0.08)[z]		7.99[s]		
Ba II $6p\ ^2P_{3/2}$	6.31 (0.016)[ee]		6.39[s]		
	6.35 (0.09)[ff]				

[a]Reference [1].
[b]Reference [8].
[c]Reference [7].
[d]Reference [40].
[e]Reference [35].
[f]Reference [36].
[g]Reference [33] (model potential).
[h]Reference [33] (close coupling).
[i]Reference [9].
[j]Reference [32].
[k]Reference [41].
[l]Reference [38].
[m]Reference [42].
[n]Reference [43].
[o]Reference [44] (HF+CI).
[p]Reference [45] (Dirac-Fock).
[q]This work.
[r]Reference [27].
[s]Reference [13].
[t]Reference [28].
[u]Reference [30].
[v]Reference [13] without semiempirical correction.
[w]Reference [29].
[x]Reference [46].
[y]Reference [47].
[z]Reference [48].
[aa]Reference [17].
[bb]Reference [11].
[cc]Reference [49].
[dd]Reference [39].
[ee]Reference [50].
[ff]Reference [2].

ations occurring for the $4p$ levels of Ca II and Cu I. Even for these cases, agreement with experiment is better than that found using *ab initio* theories.

VI. CONCLUSION

Our precise lifetime measurements on Ca II $4p\ ^2P$ levels lie above all theoretical calculations, but are in best agreement with the semiempirical calculations of Theodosiou [28]. Comparison of theory with other precise lifetime measurements for systems with a single electron outside a closed shell reveal that for systems lying lower in the Periodic Table than Sr^+, *ab initio* theory tends to fall below the experimental data, even when semiempirical corrections to the theory are used. Agreement between theory and experiment for heavier alkali-metal systems is much better, but experimental precision is lower. On the other hand, the semiempirical calculations of Theodosiou and co-workers [9,28,40] are either in excellent agreement with measurement, or are closer than other theoretical approaches.

Our measurement on the Ar II $4p'\ ^2F_{7/2}$ level [5], a system with a single hole in a closed shell, but with internal excitation, agrees with recent many-electron theory [26] at the 2% level, comparable to the agreement with theory for systems with a single electron outside a closed shell.

ACKNOWLEDGMENTS

This research was initiated and concluded with support from the National Science Foundation, and was supported continuously by the Robert A. Welch Foundation. D. A. C. expresses his appreciation to Dr. C. Guet and Dr. S. Blundell for encouraging these measurements, to Dr. A. Weiss, Dr. Y.-K. Kim, and Dr. C. F. Fischer for helpful communications, and to Dr. J. E. Hansen for communicating his unpublished calculations.

[1] A. Gaupp, R. Kuske, and H. J. Andrä, Phys. Rev. A **26**, 3351 (1982).
[2] M. L. Gaillard, D. J. Pegg, C. R. Bingham, H. K. Carter, R. L. Mlekodej, and J. D. Cole, Phys. Rev. A **26**, 1975 (1982).
[3] L. Ward, A. Wannstrom, A. Arneson, R. Hallin, and O. Vogel, Phys. Scr. **31**, 149 (1985).
[4] D. Marger and H. Schmoranzer, Phys. Lett. A **150**, 196 (1990).
[5] Jian Jin and D. A. Church, Phys. Rev. A **47**, 132 (1993).
[6] See, e.g., *Beam-Foil Spectroscopy*, edited by S. Bashkin (North-Holland, Amsterdam, 1973).
[7] W. R. Johnson, M. Idrees, and J. Sapirstein, Phys. Rev. A **35**, 3218 (1987).
[8] C. Froese Fischer, Nucl. Instrum. Methods B **31**, 265 (1988).
[9] C. E. Theodosiou and L. J. Curtis, Phys. Rev. A **38**, 4435 (1988).
[10] J. C. Raymond, in *Physics of Highly-Ionized Ions*, edited by R. Marrus (Plenum, New York, 1989), p. 189.
[11] S. A. Blundell, W. R. Johnson, and J. Sapirstein, Phys. Rev. A **43**, 3407 (1991).
[12] M. C. Noecker, B. P. Masterson, and C. E. Wiemann, Phys. Rev. Lett. **61**, 310 (1988).
[13] C. Guet and W. R. Johnson, Phys. Rev. A **44**, 1531 (1991).
[14] C. Froese Fischer (private communication).
[15] K. T. Chung, in *Proceedings of the Sixth International Conference on the Physics of Highly-Charged Ions*, edited by P. Richard, M. Stockli, C. L. Cocke, and C. D. Lin, AIP Conf. Proc. No. 274 (AIP, New York, 1993), p. 381.
[16] A. W. Weiss, Can. J. Chem. **70**, 456 (1992).
[17] C. E. Tanner, A. E. Livingston, R. J. Rafac, F. G. Serpa, K. W. Kukla, H. G. Berry, L. Young, and C. A. Kurtz, Phys. Rev. Lett. **69**, 2765 (1992).
[18] M. Elbel and R. Quad, Z. Naturforsch. Teil A **41**, 15 (1986).
[19] M. Elbel and R. Quad, Ann. Phys. (France) **10**, 675 (1985).
[20] D. J. Pegg, M. L. Gaillard, C. R. Bingham, H. K. Carter, and R. C. Mlekodej, Nucl. Instrum. Methods **202**, 153 (1982).
[21] C. Camhy-Val, A. M. Dumont, M. Dreaux, L. Perret, and C. Canderriest, J. Quantum Spectrosc. Radiat. Transfer **15**, 527 (1975).
[22] A. Hibbert and J. E. Hansen, J. Phys. B **22**, L347 (1989).
[23] H. Schmoranzer, P. Hartmetz, and D. Marger, J. Phys. B **19**, 1023 (1986).
[24] D. Marger and H. Schmoranzer, Phys. Lett. A **146**, 502 (1990).
[25] B. F. J. Luyken, Physica **60**, 432 (1972).
[26] J. E. Hansen (private communication of unpublished calculations).
[27] N. Vaeck, M. Godefroid, and C. Froese Fischer, Phys. Rev. A **46**, 3704 (1992).
[28] C. E. Theodosiou, Phys. Rev. A **39**, 4880 (1989).
[29] C. Laughlin, Phys. Scr. **46**, 238 (1992).
[30] R. N. Gosselin, E. H. Pinnington, and W. Ansbacher, Phys. Rev. A **38**, 4887 (1988).
[31] Jian Jin and D. A. Church, Phys. Rev. Lett. **70**, 3213 (1993).
[32] J. S. Sims, S. A. Hagstrom, and J. R. Rumble, Phys. Rev. A **13**, 242 (1976).
[33] G. Peach, H. E. Saraph, and M. J. Seaton, J. Phys. B **21**, 3669 (1988).
[34] S. A. Blundell, W. R. Johnson, Z. W. Liu, and J. Sapirstein, Phys. Rev. A **40**, 2233 (1989).
[35] J. Pipin and D. M. Bishop, Phys. Rev. A **45**, 2736 (1992).
[36] J. Carlsson and L. Sturesson, Z. Phys. D **14**, 281 (1989).
[37] H. Schmoranzer, D. Schulze-Hagenest, and S. A. Kandela (unpublished, referenced in [30]).
[38] J. Carlsson, Z. Phys. D **9**, 147 (1988).
[39] V. A. Dzuba *et al.*, Phys. Lett. A **140**, 493 (1989); **142**, 373 (1989).
[40] C. E. Theodosiou, L. J. Curtis, and M. El-Mekki, Phys. Rev. A **44**, 7144 (1991).
[41] C. Guet, S. A. Blundell, and W. R. Johnson, Phys. Lett. A **143**, 384 (1990).

[42] W. Ansbacher, Y. Li, and E. H. Pinnington, Phys. Lett. A **139**, 165 (1989).
[43] C. Froese Fischer, Can. J. Phys. **54**, 1465 (1976).
[44] S. N. Tiwary, A. P. Singh, D. D. Singh, and R. J. Sharma, Can. J. Phys. **66**, 1076 (1988).
[45] V. A. Zilitis, Opt. Spectrosc. **59**, 3 (1985).
[46] J. Carlsson, L. Sturesson, and S. Svanberg, Z. Phys. D **11**, 287 (1989).
[47] J. Carlsson, Phys. Rev. A **38**, 1702 (1988).
[48] M. Gaillard, H. J. Plohn, H. J. Andra, D. Kaiser, and H. H. Schulz, in *Beam Foil Spectroscopy,* edited by I. A. Sellin and D. J. Pegg (Plenum, New York, 1976), Vol. 2, p. 853.
[49] S. Rydberg and S. Svanberg, Phys. Scr. **5**, 209 (1972).
[50] H. J. Andrä, in *Beam Foil Spectroscopy* (Ref. [48]), Vol. 2, p. 835.